J Solid State Electrochem (2003) 8: 28–33
DOI 10.1007/s10008-003-0407-7

ORIGINAL PAPER

N. Van Landschoot · E. M. Kelder · J. Schoonman

Synthesis and characterization of $LiCo_{1-x}Fe_xVO_4$ prepared by a citric acid complex method

Received: 15 November 2002 / Accepted: 11 June 2003 / Published online: 20 August 2003
© Springer-Verlag 2003

Abstract For the first time, a method involving a citric acid complex has been used to prepare Fe-doped $LiCoVO_4$. $LiCoVO_4$ has the inverse spinel structure and posses a high voltage of 4.3 V vs. metallic Li. A disadvantage of $LiCoVO_4$ is its poor electronic conductivity, which is enhanced by using an Fe dopant. The doping levels were between 2 and 10 mol% to increase the electrical conductivity of the material. The citric acid complex method enabled us to make small particles in the range 0.3–0.6 μm. The structure and the electrochemical properties of these materials were studied using X-ray diffraction, thermal gravimetric analysis, scanning electron microscopy, cyclic voltammetry, and cycle tests.

Keywords Citric acid complex · Iron dopant · Lithium cobalt vanadate

Introduction

In recent years, the demand for portable power sources with high energy density has increased substantially, due to the development and popularity of portable electronic devices such as camcorders, cellular phones, and notebooks. The use of high-voltage materials is one way to achieve high energy densities in batteries. Currently, three high-voltage cathode materials are commercially available, i.e. (1) $LiNiO_2$, (2) $LiCoO_2$, and (3) $LiMn_2O_4$. These three cathode materials have a voltage range of 3.8–4.3 V vs. metallic Li.

Presented at the 3rd International Meeting on Advanced Batteries and Accumulators, 16–20 June 2002, Brno, Czech Republic

N. Van Landschoot (✉) · E. M. Kelder · J. Schoonman
Laboratory for Inorganic Chemistry,
Delft Institute for Sustainable Energy,
Delft University of Technology,
Julianalaan 136, 2628 BL Delft,
The Netherlands
E-mail: n.vanlandschoot@tnw.tudelft.nl

Inverse spinel materials, such as $LiNiVO_4$ and $LiCoVO_4$, with high theoretical capacities of about 148 mAh/g, have been studied intensively by Fey et al. [1, 2, 3, 4]. Both materials are very interesting as cathode materials, because of their high voltage of 4.3–4.9 V vs. metallic Li. The inverse spinel crystal structure of $LiCoVO_4$, as shown in Fig. 1, has been known since 1961; the Li^+ and Co^{2+} ions are distributed randomly on the octahedral sites (16d) of the structure and the V^{5+} ions on the tetrahedral sites (8a). Owing to the cubic close-packed structure, the inverse spinel structure offers a three-dimensional lattice for insertion and extraction of Li ions. The inverse spinel lattice has empty tetrahedral (8b, 48f) and octahedral sites (16c). The four 16d sites surround the 8b site, which is the Li-ion hopping pathway for inverse spinels. Recently, Liu et al. [8] showed for Li_xNiVO_4, with $x > 1$, that all the Li ions will occupy the octahedral sites and that mutual chemical substitution between V and Ni was found. Arrabito et al. [5] showed that 37.5% of V ions in the $LiNiVO_4$ system are located on octahedral positions, which have been substituted for the Ni ions in the structure, according to solid-state ^{51}V NMR. This 3d transition metal interchange then blocks the electronic pathway in these inverse spinels. However, Arrabito et al. [5] also found that within the $LiCoVO_4$ structure the V ions are only distributed on the tetrahedral sites. Landschoot et al. [6] found that poor electronic conductivity even resulted from a new inverse spinel phase upon Li extraction for $LiCoVO_4$. The Li ions in $LiCoVO_4$ could be extracted only from the outer shell of the particle, creating a fast Li-ion migration path at the surface of this particle compared to slow migration in the bulk. Landschoot et al. [7] also found that with the use of a 3d dopant, e.g. Cu, Cr, or Fe, the electrical conductivity as well as the capacity increases as a result of these dopants.

The use of a citric acid complex method enabled us to produce small particles, allowing us to increase the surface area for Li-ion extraction and reduce both the synthesis temperature and the firing time. This reduction in both the temperature and firing time is an economically

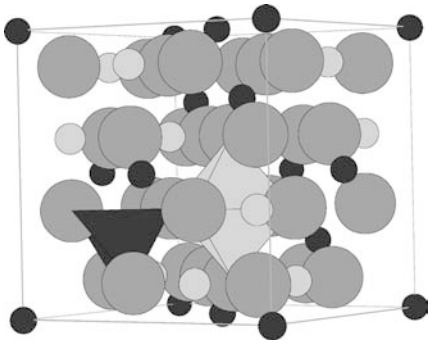

Fig. 1 The inverse spinel structure. O^{2-} (32e): *large grey spheres*; V^{5+} (8a): *small dark spheres*; Co^{2+}/ Li^{+} (16d): *small light spheres*. A *dark tetrahedron* (V) and a *light octahedron* (Li/Co) have been added to the figure

interesting method to produce the powder compared to conventional solid-state methods.

Landschoot et al. [7] showed that the use of a dopant improved the electrical conductivity and increased the cycle efficiency of $LiCoVO_4$. Our hypothesis is that by combining both the use of a dopant and having a nano-structured powder we will be able to reversibly extract more Li ions from the particles.

Experimental

A series of $LiCo_{1-x}Fe_xVO_4$ complexes ($x = 0.1$, 0.08, 0.06, 0.04, 0.02) was made via a citric acid complex method. Li_2CO_3 (Baker, >99%), $CoCO_3.H_2O$ (Merck, >99%), and NH_4VO_3 (Acros Organics, >98%) were used as the precursors. As dopant, $FeCl_2.nH_2O$ was used. The starting materials, with a molar ratio of Li:V:Co:Fe = 1:1:1−*x*:*x*, were added to 100 mL of distilled water under magnetic stirring at 80 °C. A citric acid solution was slowly added to the mixed dispersion, forming a clear dark-purple solution after the reaction. During the reaction, gas evolution occurred. The solution was then held at 80 °C, forming a gel when all the water was evaporated; no gas evolution occurred. This gel was then placed in a vacuum furnace at 120 °C for 3 h. The obtained powder was fired for respectively 1 and 2 h at 550 °C in air with intermediate ball milling.

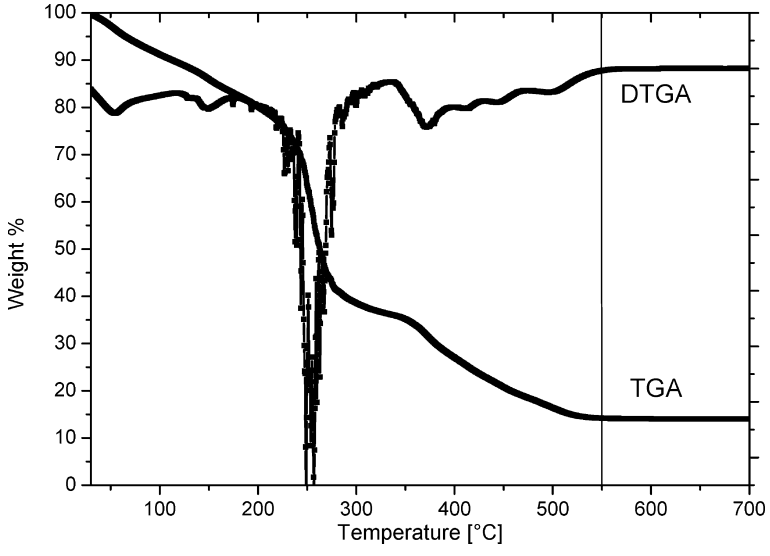

Fig. 2 TGA and DTGA curves for the $LiCo_{1-x}Fe_xVO_4$ precursor

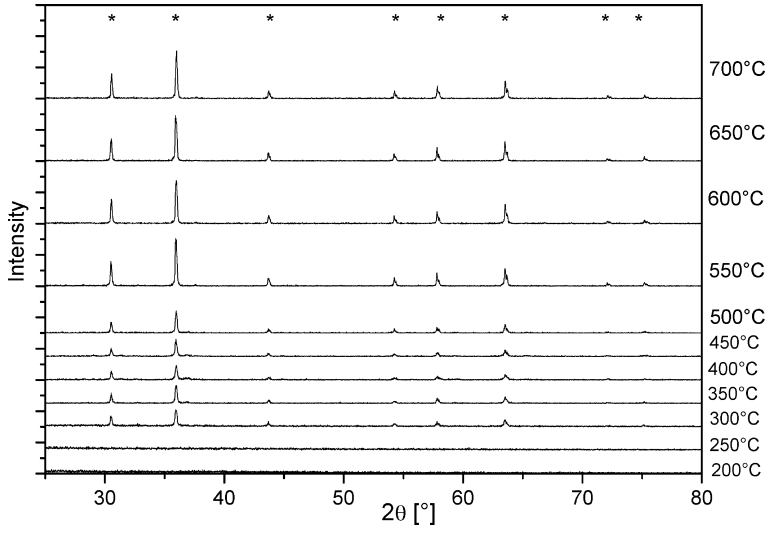

Fig. 3 XRD patterns for the $LiCo_{1-x}Fe_xVO_4$ precursor at different temperatures, in the range from 150 °C up to 700 °C. The *asterisks* indicate the different [*hkl*] reflections of $LiCo_{1-x}Fe_xVO_4$

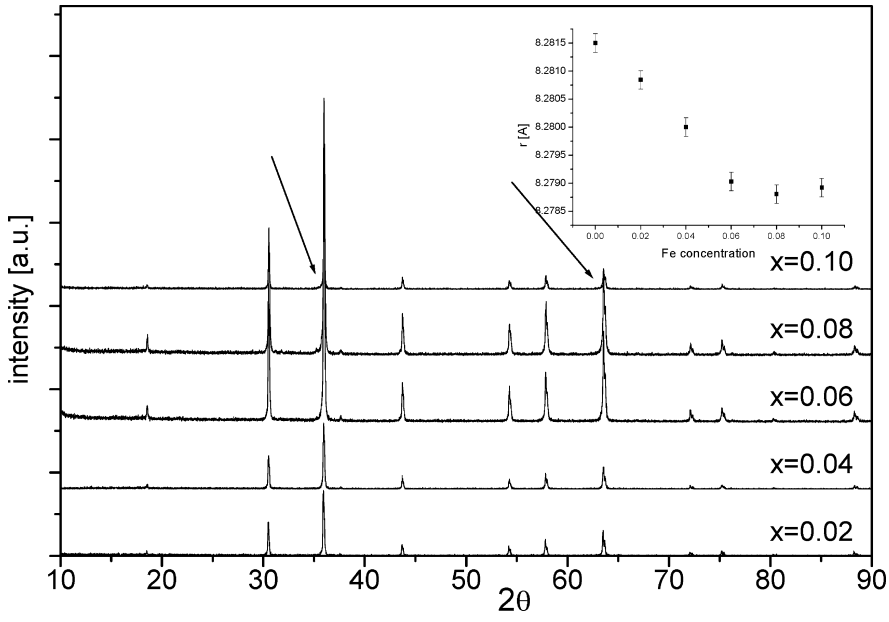

Fig. 4 XRD patterns for $LiCo_{1-x}Fe_xVO_4$ fired at 500 °C in air; the *arrows* indicate the positions of the Fe_2O_3 impurity. The lattice parameter as a function of the Fe concentration has been added to the graph

X-ray diffraction was used to determine the phase purity and the structure parameters of the final products using a Bruker D8 Advance X-Ray Diffractometer with Cu-K_α radiation. The X-ray powder diffraction patterns were collected at a step size of 0.02° with a step time of 1.5 s in a range of 10–90° in 2θ.. Single-phase spectra were fitted using EVA to obtain the lattice parameter using Bragg's Law. Scanning electron microscopy images were taken with a JEOL 3800LV instrument to determine the average particle size and distribution.

Thermal gravimetric analysis (TGA) measurements were carried out on a Perkin-Elmer TGA-7 analyser in air at a heating rate of 10°C/min. The temperature range was 30–700 °C.

Electrodes were made using a doctor blade technique on a 12-μm thick aluminium foil. They contain 85 wt% active material, 6 wt% carbon black, and 9 wt% PVDF. From the foil, 15 mm discs were punched out. The cells were assembled in a helium-filled glove box. The cells were tested against metallic Li charged at 0.2 mA/cm^2 and discharged at 0.2 mA/cm^2. $LiPF_6$ dissolved in EC/DMC (1:2; Mitsubishi Chemicals) was used as the electrolyte and Solupor (DSM Solutech) as the separator. The electrochemical characterization was done using CR2320 coin-type cells. The cells were cycled using a MACCOR battery tester. For the cyclic voltammetry measurements an Autolab was used with a scan speed of 0.1 mV/s between 3.0 and 4.5 V versus metallic Li.

Results and discussion

The use of carbonate groups in combination with citric acid leads to the formation of CO_2(g), H_2O, and a citric acid complex:

$$\begin{aligned} &Li_2CO_3 + 2(1-x)CoCO_3 \cdot H_2O + 2C_6H_8O_7 \\ &\quad + 2xFeCl_2 \cdot H_2O \;\rightarrow\; 2LiCo_{1-x}Fe_xC_6H_7O_7 \\ &\quad + 3CO_2\uparrow + 3H_2O + 4xHCl \end{aligned} \tag{1}$$

Adding NH_4VO_3 to the solution, V_2O_5 is formed:

$$\begin{aligned} &2NH_4VO_3 + 2C_6H_8O_7 \;\rightarrow\; V_2O_5 \\ &\quad + 2(NH_4)C_6H_7O_7 + H_2O \end{aligned} \tag{2}$$

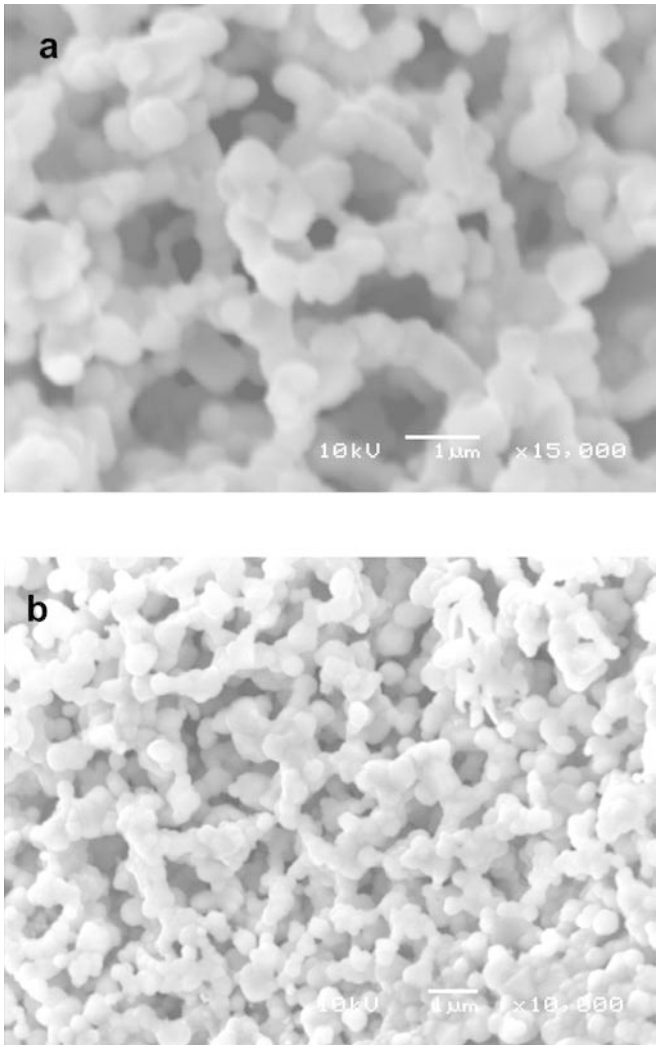

Fig. 5 (**a**) SEM image of $LiCo_{0.98}Fe_{0.02}VO_4$. (**b**) SEM image of $LiCo_{0.96}Fe_{0.04}VO_4$

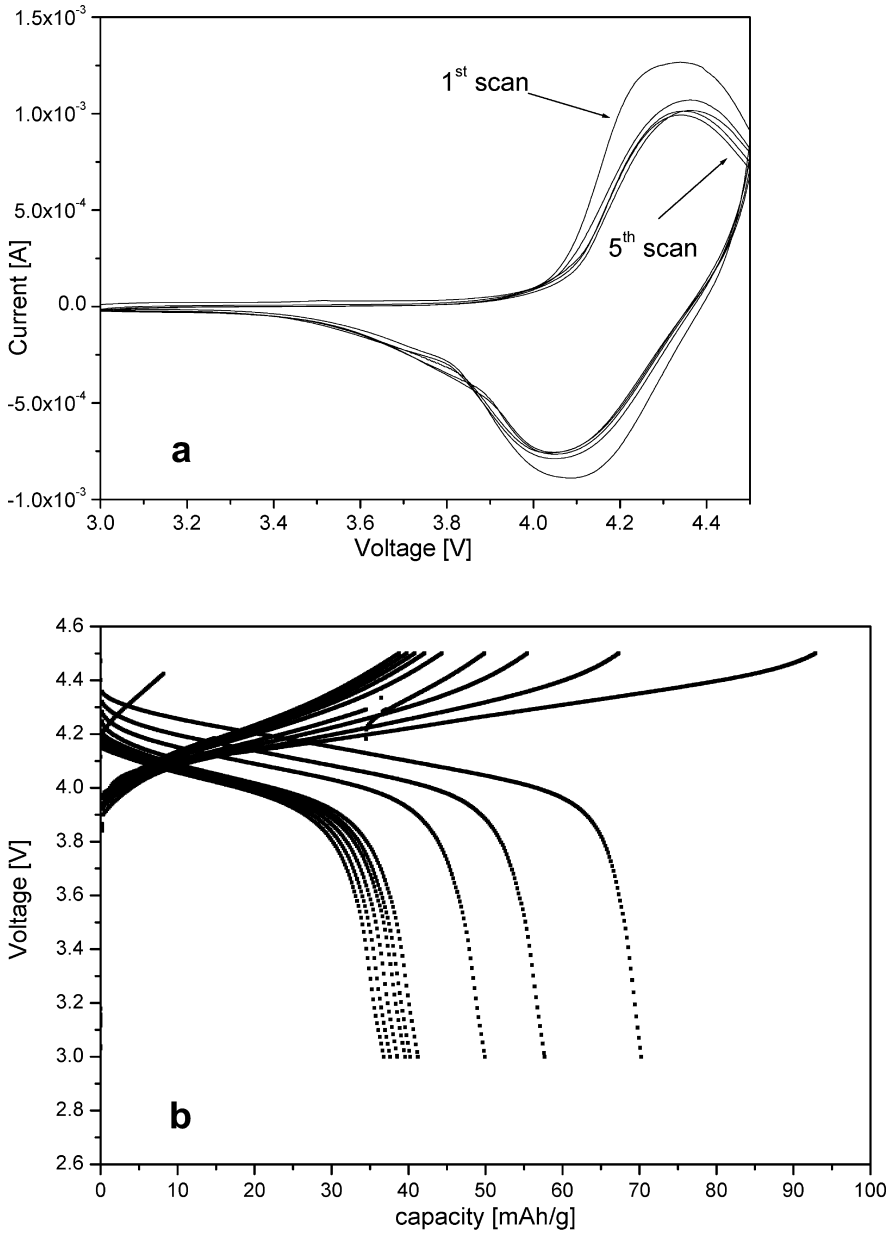

Fig. 6 (**a**) Cyclic voltammogram of $LiCo_{0.98}Fe_{0.02}VO_4$ vs. metallic Li; the scan rate was 0.2 mV/s between 3.0 and 4.5 V. (**b**) Charge/discharge graph for the first 10 cycles of $LiCo_{0.98}Fe_{0.02}VO_4$ vs. metallic Li. The charge and discharge rate was 0.1 mAh/g; the cell was cycled between 3.0 and 4.5 V

In an acidic solution, V_2O_5 reacts as an oxidant in combination with citric acid to form a $(VO)C_6H_6O_7$ complex:

$$V_2O_5 + 4C_6H_8O_7 \rightarrow 2(VO)C_6H_6O_7 + H_2O \quad (3)$$

Liu et al. [8] suggested that the dried precursor gel might be composed of $LiNiVO_4.(VO)(NH_4).C_6H_5O_7$. However, they said that the molar ratio of the starting reactants was 1:1:1 (Li:Ni:V). This does not explain the extra molar V in their precursor gel. We believe that total reaction is as follows:

$$\begin{aligned} &Li_2CO_3 + 2(1-x)CoCO_3 \cdot H_2O + 2C_6H_8O_7 \\ &\quad + 2NH_4VO_3 + 2O_2 + xFeCl_2 \cdot H_2O \\ &\quad \rightarrow 2LiCo_{1-x}Fe_xVO_4 \cdot C_6H_7O_7 + 3CO_2 \uparrow \\ &\quad + 6H_2O + 2xHCl \end{aligned} \quad (4)$$

The $LiCo_{1-x}Fe_xVO_4$ citric acid complex is formed as precursor and these finding are also proven by our TGA experiments, as shown in Fig. 2. In the temperature region 30–220 °C the observed weight loss is attributed to the removal of water and the decomposition of the excess of citric acid and other organic residues. In the temperature range 220–320 °C the decomposition of the $LiCo_{1-x}Fe_xVO_4 \cdot C_6H_7O_7$ complex occurs. This decomposition is associated with a weight loss of 45%. In this region the crystallization of $LiCo_{1-x}Fe_xVO_4$ takes place. In the temperature range 320–550 °C the decomposition of the citric acid occurs. The weight loss stops at 550 °C and the $LiCo_{1-x}Fe_xVO_4$ materials were sintered at this temperature. The supposed formation of $LiCo_{1-x}Fe_xVO_4$ between 250 °C and 300 °C is also confirmed by XRD experiments that were conducted on the precursor at different temperatures, as shown in Fig. 3.

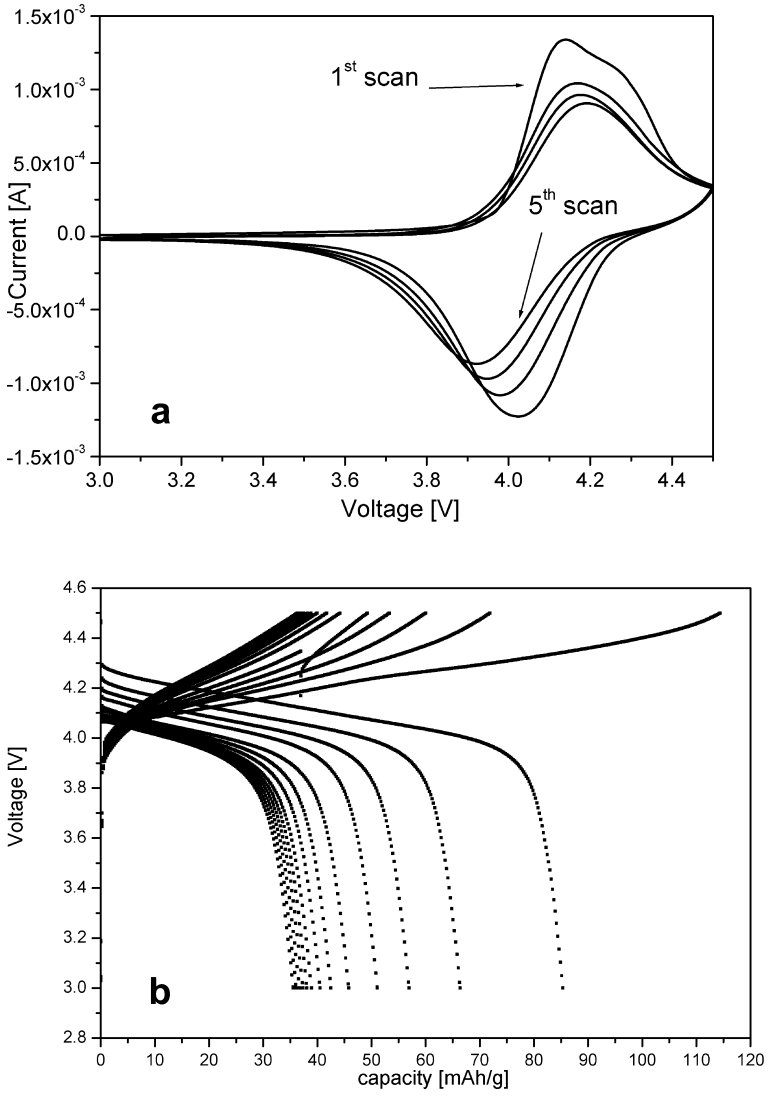

Fig. 7 (**a**) Cyclic voltammogram of $LiCo_{0.96}Fe_{0.04}VO_4$ vs. metallic Li; the scan rate was 0.1 mV/s between 3.0 and 4.5 V. (**b**) Charge/discharge graph for the first 10 cycles of $LiCo_{0.96}Fe_{0.04}VO_4$ vs. metallic Li. The charge and discharge rate was 0.2 mAh/g; the cell was cycled between 3.0 and 4.5 V

The XRD patterns show an amorphous phase up to 250 °C. At 300 °C the formation of $LiCo_{1-x}Fe_xVO_4$ appears and the patterns show an increase in the crystallinity of the material up to 600 °C.

The XRD patterns of the $LiCo_{1-x}Fe_xVO_4$ complexes ($x = 0.1$, 0.08, 0.06, 0.04, 0.02) are presented in Fig. 4. This figure shows that the material with Fe^{3+} dopant levels of 0.08 mol% and 0.10 mol% show Fe_2O_3 as an impurity, as indicated by the arrow in the graph. The other powders are phase pure and still exhibit the inverse spinel structure (*Fd3m*). For the Fe^{3+}-doped powders the lattice parameter decreases from 8.281 Å to 8.2798 Å for the Fe-doped samples. From previous work we have shown that the Fe^{3+} dopants are located on the octahedral sites. For the electrochemical tests, only the phase-pure materials were tested.

Figure 5 represents SEM images of $LiCo_{0.98}Fe_{0.02}VO_4$ and $LiCo_{0.96}Fe_{0.04}VO_4$. The SEM photographs show that the particles are basically spherical but sintered and that the particle size distribution is quite narrow. The particles have an average size between 0.3 μm and 0.6 μm.

Figure 6a shows a cyclic voltammogram for $LiCo_{0.98}Fe_{0.02}VO_4$ vs. metallic Li for the first four scans. A typical voltammogram was observed for lithium insertion compounds; there is a decay in the capacity from the first cycle. This is probably due to the structural rearrangements of the material. After the initial cycle the decay becomes less. This is also shown in Fig. 6b, where the capacity is plotted as a function of the cycle number. The initial discharge capacity is 70 mAh/g, which is substantially higher than for $LiCoVO_4$. Another important observation is the enormous increase in the internal resistance of the system that increases with the cycle number. However, after six cycles the capacity has dropped to 35 mAh/g; this phenomenon is also observed for $LiCoVO_4$.. The increase in the internal resistance is due to the internal diffusion of the V^{5+} ions from the tetrahedral sites towards the octahedral sites. The V^{5+} ions are blocking the reinsertion of Li ions into the structure and therefore lowering the capacity. This is also shown for $LiCo_{0.96}Fe_{0.04}VO_4$ vs. metallic Li, as illustrated in Fig. 7. Fig. 7a shows the cyclic voltammogram for $LiCo_{0.96}Fe_{0.04}VO_4$ vs. metallic Li. The first

cathodic scan shows two peaks that disappear after a few cycles. This is also observed for the anodic scan. These two intercalation peaks are also noted during the cycle test shown in Fig. 7b and disappear after prolonged cycling. We believe that the dopant has increased the electronic conductivity of the material and therefore more Li ions could be extracted from the structure, which leads to the appearance of another intercalation peak, as seen from the CV measurements and the cycle test. However, the cycle test also showed an increase in the internal resistance to the internal rearrangements of the V^{5+} ions in the structure. We believe that due to the improved electronic properties of the material that lead to an increase of the discharge capacity the stability of the structure decreased and that this therefore leads to a decrease of the performance.

Conclusions

The use of a citric acid complex method enabled us to produce small particles, allowing us to increase the surface area for Li-ion extraction and reduce both the firing temperature and the firing time.

The use of an Fe dopant proved that in the first cycles the capacity had indeed increased. Nevertheless, the capacity dropped after six cycles to 35 mAh/g. This phenomenon is ascribed to the internal rearrangement of V^{5+} ions from tetrahedral positions towards octahedral positions and therefore blocking the pathway of both electrons and Li ions to migrate through the structure. The improved electronic properties of the material lead to an increase of the initial charge and discharge capacity of the Fe^{3+}-doped material. However, the stability of the structure decreased and this leads to a decrease of the performance.

Acknowledgements The Delft Institute for Sustainable Energy is acknowledged for financial support. The authors would like to thank Mr. W. Rittel and Mr. P.R. Venema for assistance in the preparation and characterization of the materials. DSM Solutech is gratefully acknowledged for providing the separator material.

References

1. Fey GTK, Huang D, Gray F (1999) Electrochim Acta 45:295
2. Fey GTK, Wang KS, Wang SM (1997) J Power Sources 68:159
3. Fey GTK, Wu C (1997) Pure Appl Chem 69:2329
4. Fey GTK, Li W, Dahn JR (1994) J Electrochem Soc 141:2279
5. Arrabito M, Bodoardo S, Penazzi N, Panero S, Reale P, Scrosati B, Wang Y, Guo X, Greenbaum SG (2001) J Power Sources 97–98:478
6. Van Landschoot N, Kelder EM, Schoonman J (2001) ITE Lett Batteries New Technol Med 2:88
7. Van Landschoot N, Kelder EM, Schoonman J (2003) J Electrochem Soc (in press)
8. Liu J-R, Wang M, Lin X, Yin DC, Huang W-D (2002) J Power Sources 108:113